



Cite this: *Org. Chem. Front.*, 2015, 2, 340

## *N*-Alkyl ammonium resorcinarene salts: multivalent halogen-bonded deep-cavity cavitands†

N. Kodiah Beyeh,<sup>\*a</sup> Arto Valkonen,<sup>a,b</sup> Sandip Bhowmik,<sup>a</sup> Fangfang Pan<sup>a</sup> and K. Rissanen<sup>\*a</sup>

*N*-Cyclohexyl ammonium resorcinarene halides, stabilized by an intricate array of hydrogen bonds in a cavitand-like assembly, form multivalent halogen-bonded deep-cavity cavitands with perfluoroiodobenzenes. As observed from the macromolar to infinite concentration range through crystal growth and single crystal X-ray analyses, four 1,4-diiodotetrafluorobenzenes form moderate halogen bonds with the bromides of the *N*-cyclohexyl ammonium resorcinarene bromides leading to a deep-cavity cavitand-like structure. In this assembly, the *N*-cyclohexyl ammonium resorcinarene bromide also acts as a guest and sits in the upper cavity of the assembly interacting with the 1,4-diiodotetrafluorobenzene through strong  $\pi \cdots \pi$  interactions. Solvent molecules act as guests and are located deep in the cavity of the resorcinarene skeleton. In the millimolar range, <sup>1</sup>H and <sup>19</sup>F NMR spectroscopic analyses confirm halogen bonding in solution. Fast exchange binding of electron rich fluorophores (naphthalene, anthracene and pyrene) in the upper layer of these assemblies was also observed in the millimolar range while in the micromolar range, using fluorescence analysis, no binding of the fluorophores was observed.

Received 12th December 2014,  
Accepted 24th January 2015

DOI: 10.1039/c4qo00326h

rsc.li/frontiers-organic

## Introduction

Multivalency is a key phenomenon in system chemistry whereby strong yet reversible interactions lead to complex and functional architectures.<sup>1,2</sup> Multivalency, which describes molecular recognition phenomena between two binding partners involving more than one binding site, is prevalent in biology and biochemistry.<sup>3,4</sup> The utilization of weak interactions in mimicking biological and covalent systems is a constant challenge in nanochemistry since in most cases the final assemblies result from a compromise between the competing weak interactions and the geometrical constraints of the building blocks.<sup>5,6</sup>

Hydrogen bonds (HBs) are arguably the most used weak interactions in the design of supramolecular architectures.<sup>6,7</sup> Recently, the halogen bond (XB) which results from a charge transfer interaction between polarized halogen atoms and

Lewis bases and is similar to the HB in terms of strength and directionality, was defined and extensively reviewed.<sup>8</sup> XBs have been widely studied in crystal engineering<sup>9–11</sup> and also in materials chemistry.<sup>12,13</sup> Receptors capable of utilizing both HBs and XBs and working cooperatively are uncommon. There are reports of several receptors that can selectively recognize anions utilizing either XBs or both HBs and XBs as a result of distinct preferences in either or both of the interactions.<sup>14</sup> A more recent report shows the recognition of oxoanions using a bis(triazolium) receptor through HBs and XBs with high stability constants.<sup>15</sup>

Resorcinarenes are very important supramolecular host systems by virtue of their ease of synthesis, the possibility for further functionalization and their interior cavities suitable for guest recognition.<sup>16,17</sup> The concave cavities of resorcinarenes in the *C*<sub>4v</sub> conformation can be utilized to bind a variety of guests through multiple weak interactions.<sup>16</sup> The aromatic rings, the phenolic hydroxyl groups and lower rims of the resorcinarenes provide a platform for further functionalization.<sup>17</sup> A six-membered ring is formed between the resorcinarenes and primary amines through Mannich condensation.<sup>18</sup> This six-membered ring can be opened in the presence of mineral acids to form *N*-alkyl ammonium resorcinarene salts.<sup>19,20</sup> These cavitand-like structures are stabilized by a strong circular intramolecular hydrogen bonded cation–anion seam formed between the –NH<sub>2</sub><sup>+</sup>–R moi-

<sup>a</sup>Department of Chemistry, P. O. Box 35, University of Jyväskylä, Finland.

E-mail: ngong.k.beyeh@jyu.fi, kari.rissanen@jyu.fi

<sup>b</sup>Department of Chemistry and Bioengineering, Tampere University of Technology, P. O. Box 541, 33101 Tampere, Finland

†Electronic supplementary information (ESI) available: X-ray analyses, <sup>1</sup>H and <sup>19</sup>F NMR and fluorescence spectroscopic data. CCDC 1038850 and 1038851. For ESI and crystallographic data in CIF or other electronic format see DOI: 10.1039/c4qo00326h



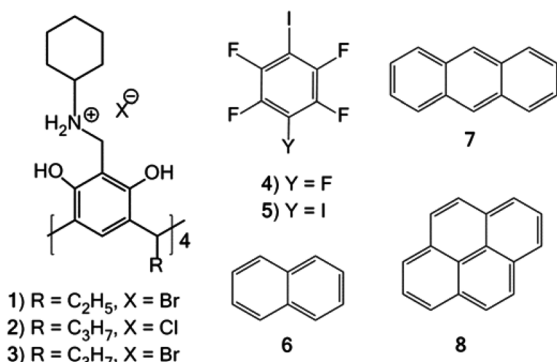


Fig. 1 *N*-Cyclohexyl ammonium resorcinarene salts 1–3, XB donors 4–5 and guests 6–8.

eties and the anions (usually halides). Chlorides and bromides are optimum for maintaining the  $C_{4v}$  symmetric nature of these large organic salt compounds through their size, and electronic and HB acceptor affinities.<sup>21</sup>

In this contribution, we present the formation of halogen-bonded deep-cavity cavitands between *N*-cyclohexyl ammonium resorcinarene halides 1–3, and perfluoroiodobenzenes 4–5 (Fig. 1). The effect of guest binding through  $\pi\cdots\pi$  interactions at different concentrations (macromolar/infinite, millimolar and micromolar) is analyzed. The guest compounds include naphthalene 6, anthracene 7, and pyrene 8 (Fig. 1). In the solid state, the aromatic regions of resorcinarene 1 act as a guest, and sit in the upper cavity of the XB assembly (Fig. 3). These assemblies are analyzed in the solid state through single crystal X-ray diffraction studies and supplemented in solution through NMR and fluorescence spectroscopic studies.

## Results and discussion

### X-Ray crystallography

Three *N*-cyclohexyl ammonium resorcinarene chloride and bromide salts (1–3) (Fig. 1) were synthesized according to reported procedures.<sup>19,21</sup> Single crystals of the *N*-cyclohexyl ammonium resorcinarene bromide 3 were obtained *via* slow evaporation from a mixture of ethanol (EtOH) and 1,2-dichloroethane (C<sub>2</sub>H<sub>4</sub>Cl<sub>2</sub>). In the structure EtOH·C<sub>2</sub>H<sub>4</sub>Cl<sub>2</sub>@3 the resorcinarene bromides are stacked in a head-to-tail motif with a single cavity that is filled with EtOH and C<sub>2</sub>H<sub>4</sub>Cl<sub>2</sub> molecules (Fig. 2). EtOH is located deep in the cavity of the receptor and interacts through two HBs (EtOH $\cdots$ Br<sup>−</sup> and NR'R''H<sub>2</sub><sup>+</sup> $\cdots$ OHEt) and CH $\cdots\pi$  interactions between the methyl groups and the electron-rich resorcinarene moiety. The disordered 1,2-dichloroethane is located close to the cavity edge between the cyclohexyl rings, wherein it donates weak HBs to Br<sup>−</sup> (CH $\cdots$ Br<sup>−</sup>) and to the O atom of EtOH (CH $\cdots$ O).

Co-crystallization of resorcinarene bromide 1 and a slight excess of 1,4-diiodotetrafluorobenzene 5 in CHCl<sub>3</sub> resulted in single crystals of the assembly CHCl<sub>3</sub>@[1·(5)<sub>4</sub>] (Fig. 3), ana-

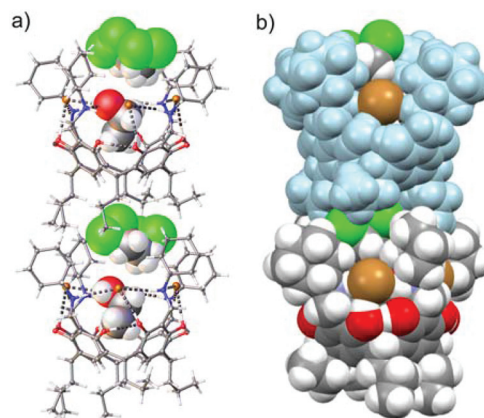


Fig. 2 Head-to-tail arrangement in the solvate crystal structure EtOH·C<sub>2</sub>H<sub>4</sub>Cl<sub>2</sub>@3: (a) ball and stick presentation with the solvent guests in CPK, (b) CPK presentation.

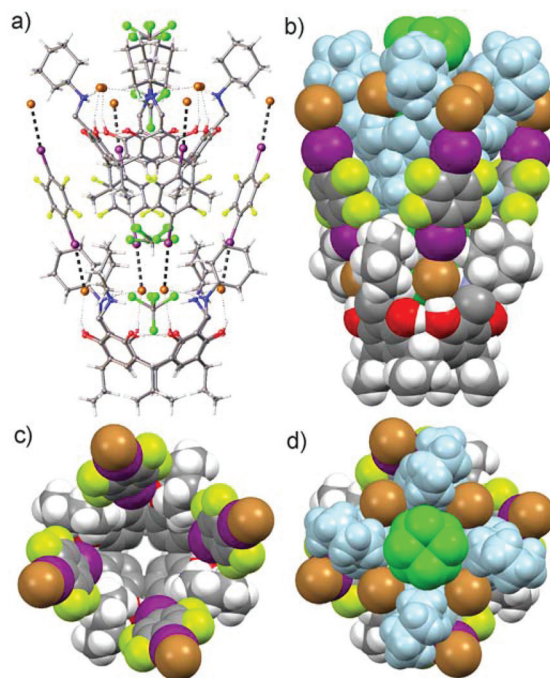


Fig. 3 Crystal structure of halogen-bonded deep-cavity cavitand CHCl<sub>3</sub>@[1·(5)<sub>4</sub>]. The disordered CHCl<sub>3</sub> molecule sits deep in the cavity of the assembly. A second resorcinarene molecule is self-included in the upper cavity of the assembly and interacts through strong  $\pi\cdots\pi$  stacking between the electron-poor phenyl rings of 5 and the electron-rich phenyl rings of the resorcinarene 1, resulting in an assembly that could be described as [CHCl<sub>3</sub> + 1]@[1·(5)<sub>4</sub>], extending into a polymeric herring-bone or cup-pile arrangement.

lyzed using X-ray crystallography. In the structure CHCl<sub>3</sub>@[1·(5)<sub>4</sub>], the strong circular HB seam ( $\cdots$ NR'R''H<sub>2</sub><sup>+</sup> $\cdots$ Br<sup>−</sup> $\cdots$ NR'R''H<sub>2</sub><sup>+</sup> $\cdots$ Br<sup>−</sup> $\cdots$ )<sub>2</sub> maintains the cavitand-like structure.<sup>19,21</sup> Anions being good Lewis bases are also suitable XB acceptors. Four molecules of 5 are halogen bonded to the bromide anions resulting in an analogue of a deep cavity cavitand (Fig. 3).<sup>22</sup> The 1,4-diiodotetrafluorobenzene 5 molecules are bound in



the open space between the cyclohexyl rings of the resorcinarene tetracation *via* both  $\text{Br}^- \cdots \text{IC}_6\text{F}_4\text{I}$  XBs and van der Waals ( $\text{IC}_6\text{F}_4\text{I}$ ) $\cdots$ cyclohexyl interactions. The interaction ratio  $R_{\text{XB}}$  ( $R_{\text{XB}} = d_{\text{XB}} / (X_{\text{vdw}} + B_{\text{vdw}})$ )<sup>23,24</sup> can be used as a rough measure of the strength of the halogen bonds. The  $R_{\text{XB}}$  ratios between 0.7–0.8 can be regarded as “strong” XBs, while those between 0.8–0.9 and 0.9–1.0 are “moderate” and “weak”, respectively. The four  $\text{I} \cdots \text{Br}^-$  halogen bonds are relatively short (3.25 Å) resulting in the XB ratio  $R_{\text{XB}} = 0.85$  with an  $\text{C}-\text{I} \cdots \text{Br}^-$  angle of 170.28° thus demonstrating a moderate XB acceptor character of the large organic salts (Fig. 3). The halogen-bonded  $\text{IC}_6\text{F}_4\text{I}$  molecules together with the cyclohexyl rings form a wall on the upper rim thus resulting in a deep cavity. The height of the cavity is *ca.* 14.90 Å, defined by the centroid-to-centroid distance of the four aromatic hydrogens on the lower rim and the four uppermost iodines of the halogen-bonded  $\text{IC}_6\text{F}_4\text{I}$  molecules. The effective diameter of the upper cavity in  $\text{CHCl}_3@[\mathbf{1} \cdot (\mathbf{5})_4]$ , defined by the closest van der Waals surfaces between the opposite uppermost iodine atoms of the  $\text{IC}_6\text{F}_4\text{I}$  molecules, is *ca.* 15.76 Å. The solvent accessible cavity void volume was calculated to be *ca.* 644.16 Å<sup>3</sup> (see ESI†).

A disordered  $\text{CHCl}_3$  molecule is located in the cavity of  $\text{CHCl}_3@[\mathbf{1} \cdot (\mathbf{5})_4]$  which is split over two positions. One part of  $\text{CHCl}_3$  at the bottom of the cavity has one C–Cl bond on the four-fold symmetry axis with another two Cl atoms averagely situated above the four positions due to the four-fold symmetry, while another part of the disordered  $\text{CHCl}_3$  molecule sits in the middle of the cavity. The three C–Cl bonds are rotating around the four-fold axis, which can be observed in 8 positions. The cavity is large enough for the lower half of another resorcinarene moiety to barge into the upper cavity position of the halogen-bonded assembly. Thus, each  $\text{CHCl}_3@[\mathbf{1} \cdot (\mathbf{5})_4]$  assembly acts as a pocket for the next assembly resulting in a polymeric herringbone or cup-pile arrangement in one direction (Fig. 3). The arrangement is stabilized *via* four relatively strong  $\pi \cdots \pi$  interactions between the electron-rich phenyl rings of **1** in the guest assembly and the electron-poor phenyl rings of **5** in the host assembly with the closest phenyl ring centroid-to-centroid distance of 4.68 Å (centroid-to-centroid for the benzene dimers is 4.96 Å).

The other iodine ends of the four XB donors  $\text{IC}_6\text{F}_4\text{I}$  in the  $\text{CHCl}_3@[\mathbf{1} \cdot (\mathbf{5})_4]$  assembly are each halogen bonded to the bromides of the next assembly in the opposite direction forming  $\text{Br}^- \cdots \text{IC}_6\text{F}_4\text{I} \cdots \text{Br}^-$  XB systems and resulting in a 3-D polymeric arrangement resembling an egg-crate-like supramolecular network (Fig. 4). The tightly packed supramolecular network looks like a pile of egg crates (Fig. 4c).

### NMR spectroscopy

The strong  $\pi \cdots \pi$  interactions between the  $\pi$ -rich surface of the resorcinarene skeleton of one receptor interacting with the  $\pi$ -poor surface of the XB donor  $\text{IC}_6\text{F}_4\text{I}$  prompted us to investigate the possibility of these halogen-bonded supramolecular structures to form host–guest complexes with electron-rich guests **6–8**. Solvent interference makes demonstrating halogen bonding in solution a rather tedious and sometimes elusive

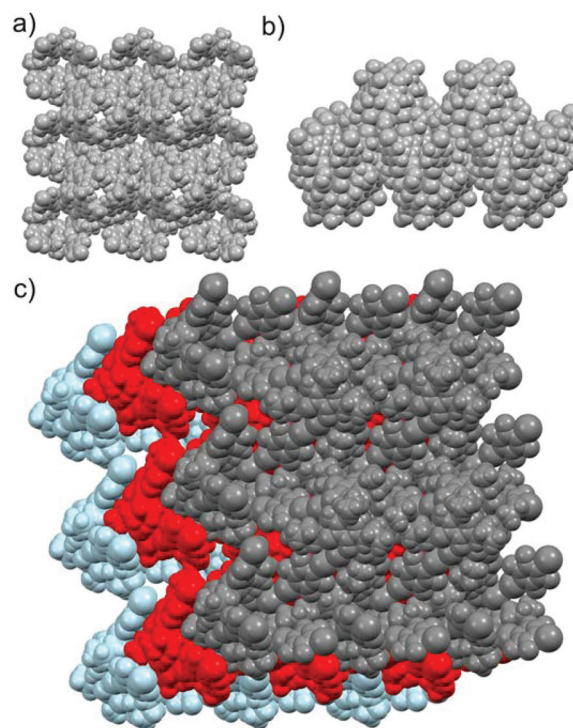


**Fig. 4** Top view (a) and side view (b) of a partial packing diagram of the complex assembly  $\mathbf{1} \cdot (\mathbf{5})_4$  resembling an egg-crate. (c) The packing of the 3-D supramolecular network looking like a pile of egg crates.

process. However, recent reports have shown NMR spectroscopy to be the most effective tool to study halogen bonding in solution.<sup>25–28</sup> Though <sup>19</sup>F NMR is suitable for halogen bonding involving perfluorinated compounds, comparative monitoring<sup>25,29</sup> of <sup>1</sup>H NMR chemical shift changes has been utilized for the detection of XB formation.<sup>25</sup> Single crystal analyses clearly show the halogen-bonded deep-cavity cavitands, resulting from an infinite concentration range in the solid state. These assemblies were then probed in the millimolar concentration range in solution *via* a series of NMR analyses.

In the experiment, several samples containing the resorcinarene hosts **2–3** and the XB donors **4–5** in a 1:4 ratio with concentrations of *ca.* 30 mM were prepared, and their <sup>1</sup>H and <sup>19</sup>F NMR spectra were recorded at 303 K in  $\text{CDCl}_3$ . The –OH and –NH<sub>2</sub> groups of the hosts are involved in the strong HB seam including the halides. The formation of XBs with the halides will thus change the electronic environment and therefore have a synergetic effect on the –OH and –NH<sub>2</sub> protons. Indeed, distinct changes in the –OH and –NH<sub>2</sub> signals were observed, thus confirming the existence of XBs in solution under these conditions (Fig. 5I, ESI†). <sup>19</sup>F NMR analysis was also utilized to further probe the existence of halogen bonding in solution. Resonance changes as a result of the formation of XBs of the –CF protons of **4** and **5** in the presence of **2** and **3** in a 4:1 ratio were observed (Fig. 5II, III). It is then concluded that the XB system that was clearly observed in the solid state at an infinite concentration is also observed in solution at a concentration of *ca.* 30 mM.



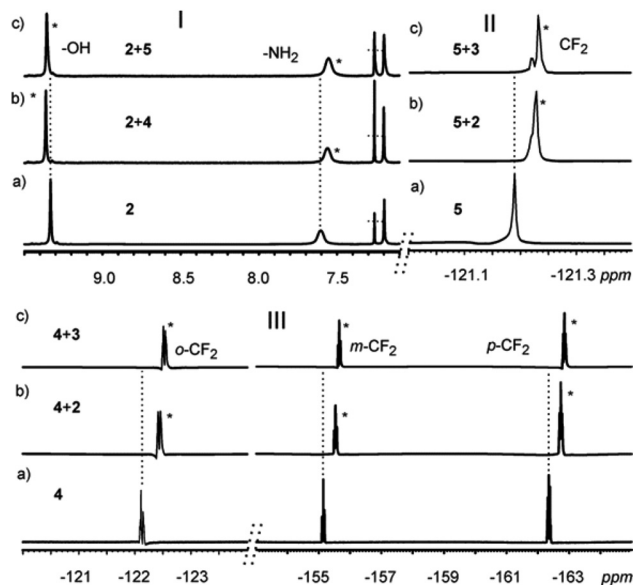


**Fig. 5** I:  $^1\text{H}$  NMR spectra (in  $\text{CDCl}_3$  at 303 K) of: (a) 2 (30 mM), (b) a 1 : 4 mixture of 2 and 4, and (c) a 1 : 4 mixture of 2 and 5. II:  $^{19}\text{F}$  NMR of: (a) 5 (30 mM), (b) a 4 : 1 mixture of 5 and 2, and (c) a 4 : 1 mixture of 5 and 3. III:  $^{19}\text{F}$  NMR spectra of: (a) 4 (30 mM), (b) a 4 : 1 mixture of 4 and 2, (c) a 4 : 1 mixture of 4 and 3.

The X-ray structure clearly shows  $\pi\cdots\pi$  interactions between the electron-poor  $\pi$ -surface of the XB donor  $\text{IC}_6\text{F}_4\text{I}$  5 and the electron-rich  $\pi$ -surface of the phenyl rings of the resorcinarene skeleton. We then proceeded to investigate the possibility of these assemblies to similarly bind electron-rich phenyl rings of the guests 6–8.  $^1\text{H}$  and  $^{19}\text{F}$  NMR measurements of a series of samples containing one of the hosts 2–3, one of the XB donors 4–5 and one of the aromatic guests 6–8 with electron-rich  $\pi$ -surfaces, in a 1 : 4 : 2 ratio, were carried out. It is generally difficult to observe  $\pi\cdots\pi$  interactions in solution at low concentrations. Since the main driving force is the  $\pi\cdots\pi$  interaction between the guests 6–8 and the XB donor situated at the upper end of the cavity of the XB deep-cavity cavitand, it is thus expected that the binding process will be very fast on the NMR timescale.

Minor upfield shifts of the  $^1\text{H}$  NMR resonances of the guest protons were observed in the samples and attributed to  $\pi\cdots\pi$  interactions. Changes in the -OH and -NH<sub>2</sub> signals of the host also confirm interactions between the host and the guest (Fig. 6 & 7, ESI<sup>†</sup>). The guests 6–8 present in the upper cavity of the assembly interact with the XB donors 4–5 and thus affect their XB interactions with the host halides resulting in synergistic changes to the -OH and -NH<sub>2</sub> signals.  $^{19}\text{F}$  NMR analysis of these samples also shows minor changes in the -CF<sub>2</sub> signals in the presence of the guests (Fig. 8, ESI<sup>†</sup>).

### Fluorescence spectroscopy

As aromatic fluorophores 6–8 were used as guests for the studies, it was imperative to look for evidence of host–guest interactions using fluorescence spectroscopy. However, to eliminate the possibility of excimer formation (and loss of

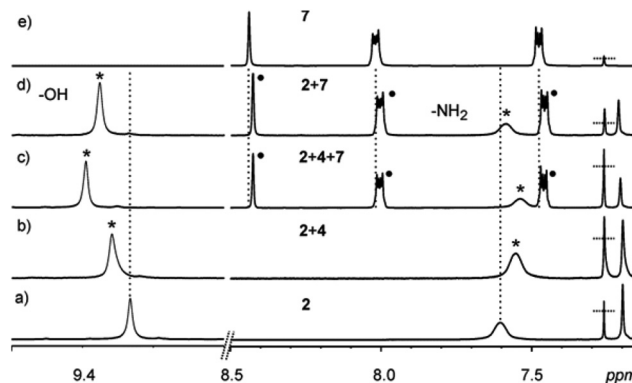


**Fig. 6**  $^1\text{H}$  NMR spectra (in  $\text{CDCl}_3$  at 303 K) of: (a) 2 (30 mM), (b) a 1 : 4 mixture of 2 and 4, (c) a 1 : 4 : 2 mixture of 2, 4 and 7, (d) a 1 : 2 mixture of 2 and 7, and (e) 7 (30 mM).

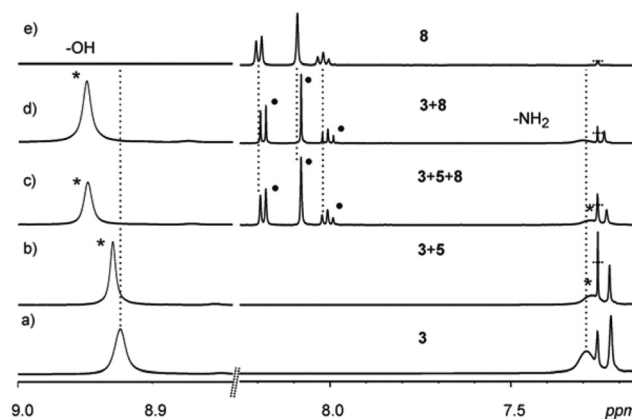


**Fig. 7**  $^1\text{H}$  NMR spectra (in  $\text{CDCl}_3$  at 303 K) of: (a) 3 (30 mM), (b) a 1 : 4 mixture of 3 and 5, (c) a 1 : 4 : 2 mixture of 3, 5 and 8, (d) a 1 : 2 mixture of 3 and 8, and (e) 8 (30 mM).

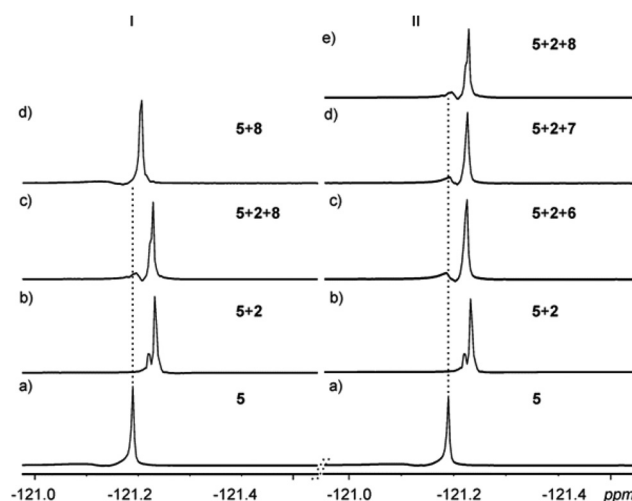


**Fig. 8** I:  $^{19}\text{F}$  NMR spectra (in  $\text{CDCl}_3$  at 303 K) of: (a) 5 (30 mM), (b) a 4 : 1 mixture of 5 and 2, (c) a 4 : 1 : 2 mixture of 5, 2 and 8, and (d) a 1 : 1 mixture of 5 and 8. II:  $^{19}\text{F}$  NMR spectra of: (a) 5 (30 mM), (b) a 4 : 1 mixture of 5 and 2, (c) a 4 : 1 : 2 mixture of 5, 2 and 6, (d) a 4 : 1 : 2 mixture of 5, 2 and 7, and (e) a 4 : 1 : 2 mixture of 5, 2 and 8.



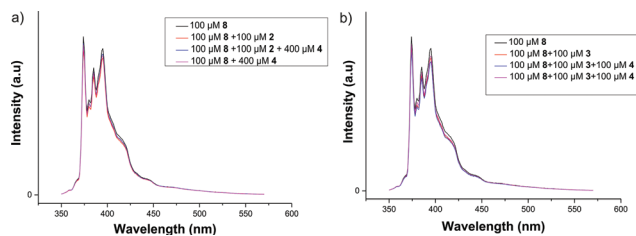


**Fig. 9** Fluorescence spectra of **8** (100  $\mu\text{M}$ ) in the presence of **4** (400  $\mu\text{M}$ ) and (a) **2** (100  $\mu\text{M}$ ) or (b) **3** (100  $\mu\text{M}$ ) in  $\text{CHCl}_3$ .  $\lambda_{\text{ext}} = 330 \text{ nm}$ .

vibrational fine structure), the emission studies were carried out at micromolar concentrations.<sup>30,31</sup> Unfortunately, no considerable changes in the fluorescence spectra of pyrene were observed in the presence of the host (2–3) and the XB donor **4** (Fig. 9). The constant  $I_1/I_3$  ratio also indicated that there has been little or no change in the pyrene environment<sup>30,31</sup> even in the presence of cavitand hosts. However, it should be noted that even at much higher concentrations (millimolar), only very weak host–guest interactions were observed in the NMR studies. Considering the various competitive equilibria/interactions in solution, the formation of host–guest complexes at micromolar concentrations would have been extremely difficult and hence was not reflected in any significant changes in the fluorescence spectra of pyrene or any of the other guests 6–7 (see ESI†).

## Conclusions

In conclusion, we present examples of HBs and XBs working in tandem in a cooperative manner to form analogues of deep-cavity cavitands between *N*-cyclohexyl ammonium resorcinarene halides and perfluoriodobenzenes 4–5. X-ray crystallography confirms moderate XBs between the XB donor **5** and the bromide acceptor in the resorcinarene salt **1**. These results show the formation of an analogue of a deep-cavity cavitand, with a larger cavity size, larger than those of some reported covalent deep-cavity cavitands.<sup>32</sup> The lower rim of the resorcinarene is located in the upper cavity of the halogen-bonded assembly acting as a guest and held together by strong  $\pi \cdots \pi$  interactions between the electron-poor ring of the XB donor **5** and the electron-rich phenyl ring of the resorcinarene skeleton **1**. The ability of NMR spectroscopy to reliably detect nucleus specific information and thermodynamic information,<sup>26</sup> was used to probe the existence of XBs in solution *via* a series of  $^1\text{H}$  and  $^{19}\text{F}$  NMR analyses. The presence of guest molecules with electron-rich  $\pi$ -surfaces did not dissociate the assemblies and even showed a fast host–guest exchange process at the millimolar concentration level. The XB process was determined to be concentration dependent as no changes were observed from several mixtures of the resorcinarene salts 2–3, the XB donors 4–5 and the guests 6–8 at the micromolar range through fluorescence measurements. Though perfluorinated iodocompounds are known to be good XB donors, the resorcinarene salts are proving to be suitable multivalent XB accep-

tors and careful organization of the components at suitable concentrations can lead to more sophisticated functional supramolecular architectures.

## Acknowledgements

The authors kindly acknowledge the Academy of Finland (KR.: no. 265328 and 263256, NKB: no. 258653), the University of Jyväskylä and the Tampere University of Technology for financial support.

## Notes and references

- G. von Kiedrowski, S. Otto and P. Herdewijn, *J. Syst. Chem.*, 2010, **1**, 1.
- A. Camara-Campos, D. Musumeci, C. A. Hunter and S. Turega, *J. Am. Chem. Soc.*, 2009, **131**, 18518.
- C. A. Hunter and H. L. Anderson, *Angew. Chem., Int. Ed.*, 2009, **48**, 7488.
- C. A. Hunter, N. Ihekweba, M. C. Misuraca, M. D. Segarra-Maset and S. M. Turega, *Chem. Commun.*, 2009, 3964.
- J.-M. Lehn, *Pure Appl. Chem.*, 1994, **66**, 1961.
- M. M. Conn and J. Rebek Jr., *Chem. Rev.*, 1997, **97**, 1647.
- G. R. Desiraju, *Angew. Chem., Int. Ed. Engl.*, 1995, **34**, 2311.
- (a) G. R. Desiraju, P. S. Ho, L. Kloo, A. C. Legon, R. Marquardt, P. Metrangolo, P. Politzer, G. Resnati and K. Rissanen, *Pure Appl. Chem.*, 2013, **85**, 1711; (b) K. Rissanen, *CrystEngComm*, 2008, **10**, 1107; (c) L. Brammer, G. Mínguez Espallargas and S. Libri, *CrystEngComm*, 2008, **10**, 1712; (d) E. Parisini, P. Metrangolo, T. Pilati, G. Resnati and G. Terraneo, *Chem. Soc. Rev.*, 2011, **40**, 2267.
- R. W. Troff, T. Mäkelä, F. Topic, A. Valkonen, K. Raatikainen and K. Rissanen, *Eur. J. Org. Chem.*, 2013, 1617.
- K. Rissanen, *CrystEngComm*, 2008, **10**, 1107.
- K. Raatikainen and K. Rissanen, *Chem. Sci.*, 2012, **2**, 1235.
- A. Priimägi, G. Cavallo, A. Forni, M. Gorynsztejn-Leben, M. Kaivola, P. Metrangolo, R. Milani, A. Shishido, T. Pilati, G. Resnati and G. Terraneo, *Adv. Funct. Mater.*, 2012, **22**, 2572.
- P. Metrangolo, Y. Carcenac, M. Lahtinen, T. Pilati, K. Rissanen, A. Vij and G. Resnati, *Science*, 2009, **323**, 1461.
- (a) M. G. Chudzinski, C. A. McClary and M. S. Taylor, *J. Am. Chem. Soc.*, 2011, **133**, 10559; (b) S. Castro-Fernández, I. R. Lahoz, A. L. Llamas-Saiz, J. L. Alonso-Gómez, M.-M. Cid and A. Navarro-Vázquez, *Org. Lett.*, 2014, **16**, 1136; (c) S. M. Walter, F. Kniep, L. Rout, F. P. Schmidtchen, E. Herdtweck and S. M. Huber, *J. Am. Chem. Soc.*, 2012, **134**, 8507.
- F. Zapata, A. Caballero, P. Molina, I. Alkorta and J. Elguero, *J. Org. Chem.*, 2014, **79**, 6959.
- P. Timmerman, W. Verboom and D. N. Reinhoudt, *Tetrahedron*, 1996, **52**, 2663.



- 17 V. Böhmer, *Angew. Chem., Int. Ed. Engl.*, 1995, **34**, 713.
- 18 K. Airola, V. Böhmer, E. F. Paulus, K. Rissanen, C. Schmidt, I. Thondorf and W. Vogt, *Tetrahedron*, 1997, **53**, 10709.
- 19 A. Shivanyuk, T. P. Spaniol, K. Rissanen, E. Kolehmainen and V. Böhmer, *Angew. Chem., Int. Ed.*, 2000, **39**, 3497.
- 20 N. K. Beyeh, M. Cetina and K. Rissanen, *Cryst. Growth Des.*, 2012, **12**, 4919.
- 21 N. K. Beyeh, M. Cetina, M. Löfman, M. Luostarinen, A. Shivanyuk and K. Rissanen, *Supramol. Chem.*, 2010, **22**, 737.
- 22 N. K. Beyeh, M. Cetina and K. Rissanen, *Chem. Commun.*, 2014, **50**, 1959.
- 23 J. P. M. Lommerse, A. J. Stone, R. Taylor and F. H. Allen, *J. Am. Chem. Soc.*, 1996, **118**, 3108.
- 24 L. Brammer, E. A. Bruton and P. Sherwood, *Cryst. Growth Des.*, 2001, **1**, 277.
- 25 J. F. Bertrán and M. Rodríguez, *Org. Magn. Reson.*, 1979, **12**, 92.
- 26 M. Erdelyi, *Chem. Soc. Rev.*, 2012, **41**, 3547.
- 27 M. G. Sarwar, D. Ajami, G. Theodorakopoulos, I. D. Petsalakis and J. Rebek Jr., *J. Am. Chem. Soc.*, 2013, **135**, 13672.
- 28 T. M. Beale, M. G. Chudzinski, M. G. Sarwar and M. Taylor, *Chem. Soc. Rev.*, 2013, **42**, 1667.
- 29 J. F. Bertrán and M. Rodríguez, *Org. Magn. Reson.*, 1980, **14**, 244.
- 30 J. Ferguson, *J. Chem. Phys.*, 1965, **43**, 306.
- 31 H. Xing, P. Yan and J. Xiao, *Soft Matter*, 2013, **9**, 1164.
- 32 K. Srinivasan and B. C. Gibb, *Org. Lett.*, 2007, **9**, 745.

